ORIGINAL ARTICLE

CD177 drives the transendothelial migration of Treg cells enriched in human colorectal cancer

Shouyu Ke[1,a], Yi Lei[2,a], Yixian Guo[1,a], Feng Xie[2], Yimeng Yu[2], Haigang Geng[1], Yiqing Zhong[1], Danhua Xu[1], Xu Liu[1], Fengrong Yu[1], Xiang Xia[1], Zizhen Zhang[1], Chunchao Zhu[1], Wei Ling[1], Bin Li[2] & Wenyi Zhao[1,b] (iD)

[1]Department of Gastrointestinal Surgery, Ren Ji Hospital, Shanghai Jiao Tong University School of Medicine, Shanghai, China
[2]Center for Immune-Related Diseases at Shanghai Institute of Immunology, Department of Respiratory and Critical Care Medicine of Ruijin Hospital, Department of Thoracic Surgery of Ruijin Hospital, Department of Immunology and Microbiology, Shanghai Jiao Tong University School of Medicine, Shanghai, China

Correspondence

W Ling and W Zhao, Department of Gastrointestinal Surgery, Ren Ji Hospital, Shanghai Jiao Tong University School of Medicine, Shanghai, China.
E-mail: lingwei050@163.com;
zhaowy2win@yeah.net

B Li, Center for Immune-Related Diseases at Shanghai Institute of Immunology, Department of Respiratory and Critical Care Medicine of Ruijin Hospital, Department of Thoracic Surgery of Ruijin Hospital, Department of Immunology and Microbiology, Shanghai Jiao Tong University School of Medicine, Shanghai, China.
E-mail: binli@shsmu.edu.cn

[a]Equal contributors.
[b]Lead contact: Wenyi Zhao.

Abstract

Objectives. Regulatory T (Treg) cells regulate immunity in autoimmune diseases and cancers. However, immunotherapies that target tumor-infiltrating Treg cells often induce unwanted immune responses and tissue inflammation. Our research focussed on exploring the expression pattern of CD177 in tumor-infiltrating Treg cells with the aim of identifying a potential target that can enhance immunotherapy effectiveness. **Methods.** Single-cell RNA sequencing (scRNA-seq) data and survival data were obtained from public databases. Twenty-one colorectal cancer patient samples, including fresh tumor tissues, peritumoral tissues and peripheral blood mononuclear cells (PBMCs), were analysed using flow cytometry. The transendothelial activity of CD177$^+$ Treg cells was substantiated using *in vitro* experiments. **Results.** ScRNA-seq and flow cytometry results indicated that CD177 was exclusively expressed in intratumoral Treg cells. CD177$^+$ Treg cells exhibited greater activation status and expressed elevated Treg cell canonical markers and immune checkpoint molecules than CD177$^-$ Treg cells. We further discovered that both intratumoral CD177$^+$ Treg cells and CD177-overexpressing induced Treg (iTreg) cells had lower levels of PD-1 than their CD177$^-$ counterparts. Moreover, CD177 overexpression significantly enhanced the transendothelial migration of Treg cells *in vitro*. **Conclusions.** These results demonstrated that Treg cells with higher CD177 levels exhibited an enhanced activation status and transendothelial migration capacity. Our findings suggest that CD177 may serve as an immunotherapeutic target and that overexpression of CD177 may improve the efficacy of chimeric antigen receptor T (CAR-T) cell therapy.

Keywords: CD177, migration, regulatory T cells, tumor microenvironment

INTRODUCTION

Colorectal cancer (CRC) is a common malignancy that ranks second in terms of cancer-related mortality worldwide.[1] Conventional CRC treatments include endoscopy, surgery, chemotherapy and radiotherapy.[2] Nevertheless, the therapeutic possibilities for individuals with advanced CRC, especially metastatic CRC, remain restricted.[3,4] Recently, immunotherapy has shown promising results in several solid tumor treatments.[5,6] However, its efficacy in CRC remains modest.[7,8] Investigating non-malignant cells (such as immune and stromal cells) and components of the CRC tumor microenvironment (TME) can help elucidate the mechanisms of tumor development and immunotherapy resistance.[9]

Regulatory T (Treg) cells are a subset of CD4^{+} T cells characterised by the expression of FOXP3.[10,11] They exhibit strong immunosuppressive functions and are critical for maintaining the immune balance and tissue homeostasis.[12,13] In the TME, Treg cells suppress the anti-tumor response via various cytokines (e.g. TGF-β, IL-10 and IL-35) and surface molecules (e.g. CTLA-4 and PD-L1).[13] Numerous studies have indicated that an increase in the number of Treg cells correlates with a diminished antitumor response, thereby facilitating tumor immune evasion in CRC.[14–16]

CD177, also known as human neutrophil antigen NB1 or PRV-1, is a 56–64 kDa glycosylphosphatidylinositol-anchored plasma membrane glycoprotein.[17,18] It is mainly expressed by neutrophils, neutrophilic metamyelocytes and myelocytes in 89–97% of healthy individuals.[19] The mean proportion of peripheral CD177^{+} neutrophils is approximately 50% but is upregulated in myeloid proliferative diseases, severe infections and after G-CSF stimulation.[20,21] CD177 regulates multiple neutrophil functions, including transmigration, via platelet endothelial cell adhesion molecule-1 PECAM-1.[18,21,22] Recently, Zhou *et al.* found that CD177^{+} neutrophils inhibit inflammatory bowel disease, highlighting the important role of CD177 in neutrophils.[23]

In addition to its expression on neutrophils, the expression of CD177 in Treg cells has been reported in several studies.[24,25] In 2021, Kim *et al.* demonstrated that CD177 modulates the function and homeostasis of tumor-infiltrating Treg cells in a mouse tumor model.[26] However, the properties of human CRC-derived CD177^{+} Treg cells remain to be elucidated. We demonstrated that CD177^{+} Treg cells are enriched and more likely to be activated in human CRC. Additionally, CD177 enhanced the transendothelial migration of both Treg and CD8^{+} T cells, which could be utilised to improve Treg-cell-based therapy or chimeric antigen receptor T (CAR-T) cell therapy.

RESULTS

CD177 was exclusively expressed by Treg cells, as determined by single-cell RNA sequencing

To gain insights into tumor-infiltrating lymphocytes, we first analysed the single-cell RNA sequencing (scRNA-seq) data of CRC patients (GSE108989).[27] In this database, T cells are classified into 20 subsets with distinct functions and clonalities (Figure 1a). Based on canonical markers defined in the literature, three FOXP3^{+} Treg cell clusters, CD4_10-FOXP3, CD4_C11-IL10 and CD4_C12-CTLA4, were enriched in the blood, normal mucosa and tumor samples, respectively.[27] We compared the gene list of the CD4_C12-CTLA4 cluster to those of the CD4_C11-IL10 and CD4_10-FOXP3 clusters separately. An analysis of differentially expressed genes demonstrated that CD177 was enriched in CD4_C12-CTLA4 Treg cells. This finding suggested that the CD4_C12-CTLA4 Treg cell cluster, which is thought to comprise tumor-infiltrating Treg cells, upregulates the expression of CD177 (Figure 1b and c). These results were validated using another human CRC scRNA-seq data set (GSE178341; Supplementary figure 1).[28] Within the GSE178341 data set, apart from T cells, we categorised single cells into 11 major cell clusters, including B cells and macrophages (Supplementary figure 1a–c). Among all immune cell subsets, Treg cells exhibited notably elevated expression levels of CD177 (Supplementary figure 1d and e).

CD177 expression pattern in tumor-infiltrating T cells

Flow cytometry was used to analyse the expression levels of CD177 protein across different T cell subsets in tumor, peritumor and peripheral blood mononuclear cells (PBMCs) samples from patients with CRC. The gating strategy is shown in Figure 2a. As illustrated in Figure 2b–e, CD177 was
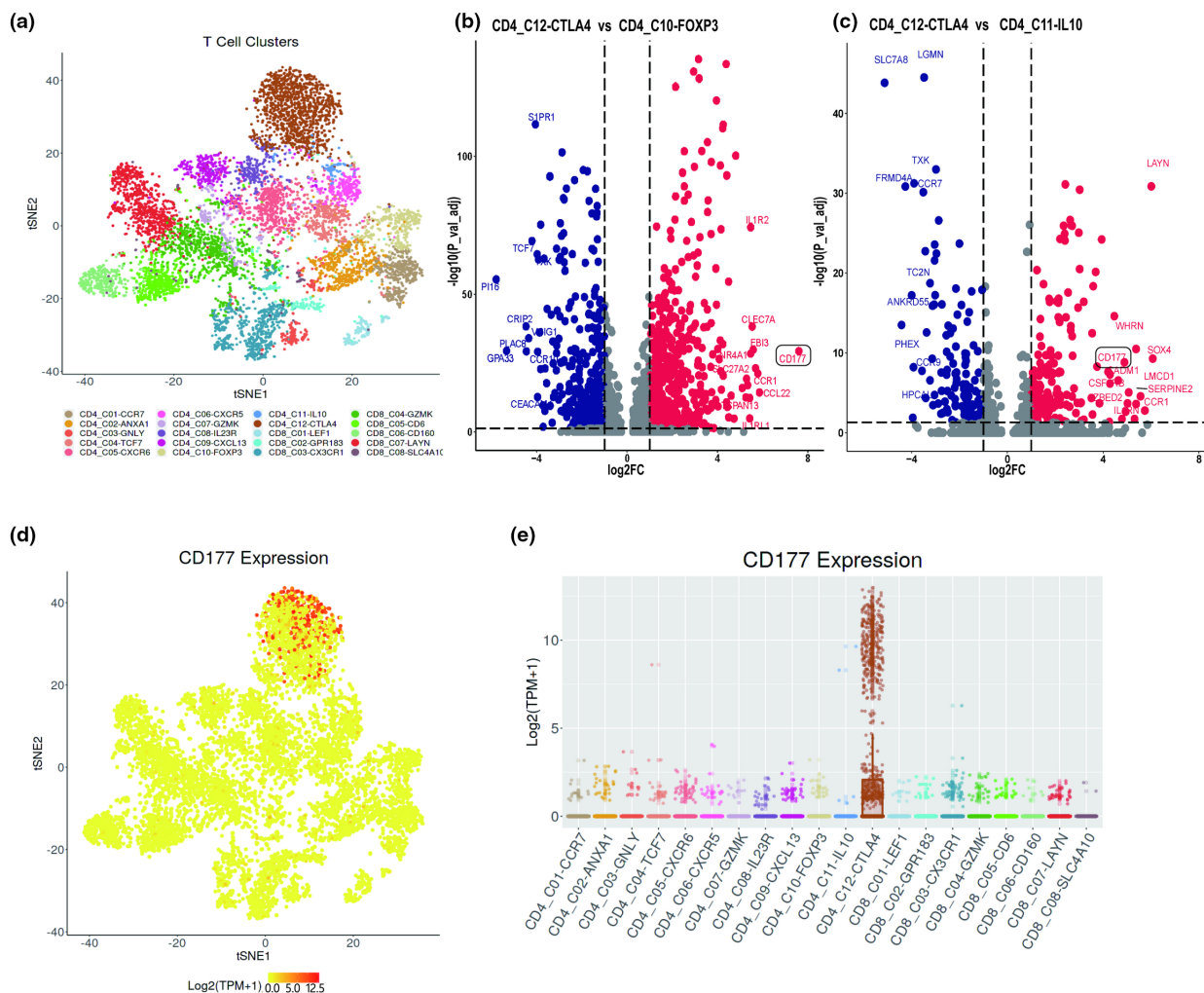
Figure 1. CD177 is exclusively expressed by tumor-infiltrating Treg cells. **(a)** tSNE plot representation of 20 unique T-cell clusters colour-coded by their corresponding subtype. Each dot in the tSNE represents one single cell. **(b)** Volcano plot shows differentially expressed genes between CD4_C12-CTLA4 (red dots) and CD4_10-FOXP3 (blue dots) clusters. **(c)** Volcano plot shows differentially expressed genes between CD4_C12-CTLA4 (red dots) and CD4_C11-IL10 (blue dots) clusters. **(d)** tSNE plot representation of CD177 expression distribution in T-cell clusters. Each dot represents one single cell, coloured by the expression level of CD177. **(e)** Box plots show the expression distribution of CD177 in T-cell clusters. Each dot represents one single cell, coloured by T-cell clusters.

highly expressed in Treg cells. Meanwhile, tumor tissues (29.29%) contained the most CD177⁺ Treg cells, followed by peritumor tissues (20.72%) and PBMCs (4.31%) (Figure 2f). In contrast, CD177 expression was minimal in CD8⁺ T and conventional CD4⁺ T (Tconv) cells (Figure 2b, g and h). Although the percentage of CD177⁺ CD8⁺ T cells in peritumor tissues was notably elevated (Figure 2h), the mean fluorescence intensity (MFI) of CD177 in CD8⁺ T cells was profoundly diminished (Supplementary figure 2a–c).

Therefore, subsequent experiments focussed on the characteristics and functions of CD177⁺ Treg cells.

Characteristics of tumor-infiltrating CD177⁺ Treg cells

Here, we investigated the features of intratumoral CD177⁺ T cells in human CRC. A schematic of the gating strategy and representative histogram plots for each marker are shown in
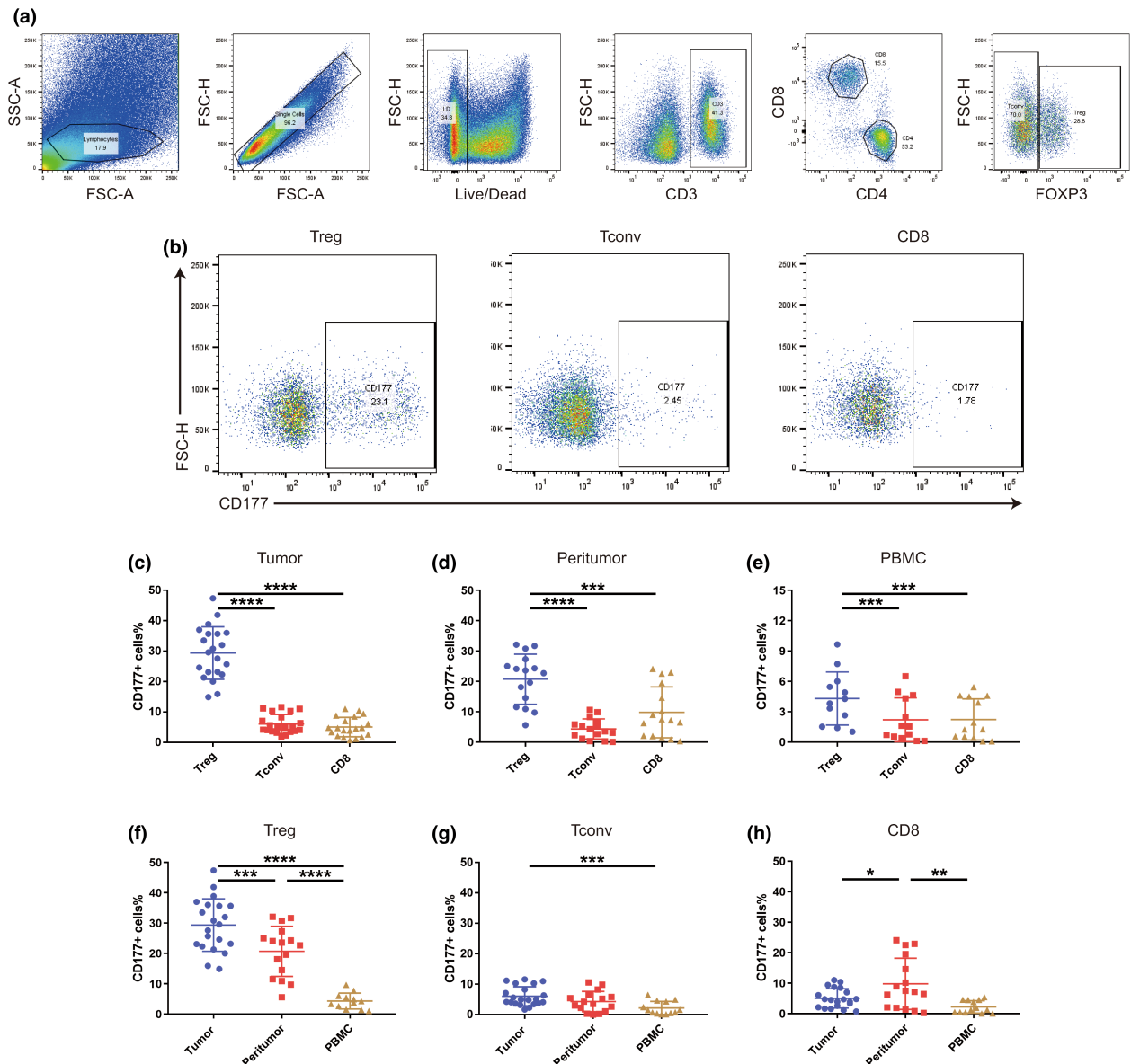
Figure 2. Expression of CD177 protein among T-cell subsets isolated from different tissues of colorectal cancer (CRC) patients. **(a)** Schematic gating strategy for the analysis of T cells from different tissues of CRC patients. Treg cell is defined as CD4+ FOXP3+ T cell and Tconv cell is defined as CD4+ FOXP3− T cell. **(b)** Schematic gating of CD177 in Treg cells (left), Tconv cells (middle), and CD8+ T cell (right) from tumor tissues of CRC patients. **(c–e)** Expression of CD177 among T cell subsets from **(c)** tumor tissues ($n = 21$), **(d)** peritumor tissues ($n = 16$) and **(e)** PBMCs ($n = 13$). **(f–h)** Expression of CD177 in Treg cells, **(g)** Tconv cells and **(h)** CD8+ T cells from different tissues. Data are represented as mean ± standard error of the mean and were analysed by one-way ANOVA **(c–h)**. *$P < 0.05$, **$P < 0.01$, ***$P < 0.001$, ****$P < 0.0001$.

Supplementary figure 3. We found that CD177+ Treg cells had higher Helios expression levels (Figure 3a), suggesting that they were more likely to be in an activated state or derived from the thymus.[29,30] CCL22, CCL19 and CCL1 are thought to play important roles in Treg cells.[31,32] The expression levels of the chemokine receptors CCR4, CCR7 and CCR8 were detected, and only CCR8 was found to be highly expressed in CD177+ Treg cells. (Figure 3b–d).

Next, we evaluated the status and function of CD177+ Treg cells. CD177+ Treg cells expressed high levels of FOXP3 and CD25, which are classical markers of Treg cells. This further indicated that
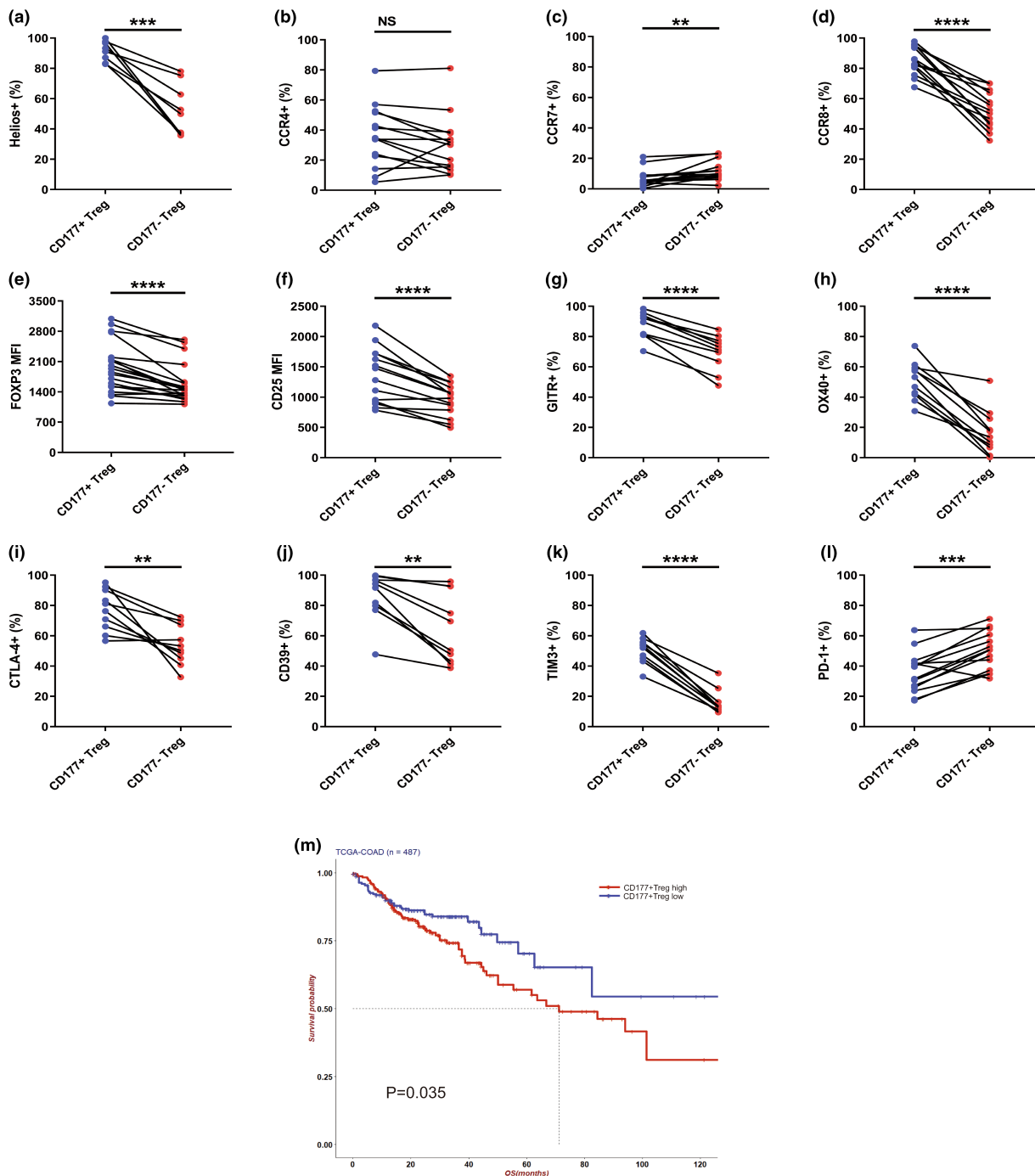
Figure 3. Characteristics of tumor-infiltrating CD177$^+$ Treg cells. **(a)** Helios expression of CD177$^+$ Treg cells and CD177$^-$ Treg cells from colorectal cancer (CRC) tissues (*n* = 8). **(b–d)** The chemokine receptors' expressions, including **(b)** CCR4 (*n* = 14), **(c)** CCR7 (*n* = 14), and **(d)** CCR8 (*n* = 14), of CD177$^+$ Treg cells and CD177$^-$ Treg cells from CRC tissues. **(e)** FOXP3 expression of CD177$^+$ Treg cells and CD177$^-$ Treg cells from CRC tissues (*n* = 21). **(f)** CD25 expression of CD177$^+$ Treg cells and CD177$^-$ Treg cells from CRC tissues (*n* = 14). **(g, h)** The immune checkpoint molecules' expressions, including **(g)** GITR (*n* = 10), **(h)** OX40 (*n* = 10), **(i)** CTLA-4 (*n* = 10), **(j)** CD39 (*n* = 10), **(k)** TIM3 (*n* = 10) and **(l)** PD-1 (*n* = 14), of CD177$^+$ Treg cells and CD177$^-$ Treg cells from CRC tissues. MFI is used to evaluate the levels of FOXP3 and CD25. The positive percentage is used to evaluate the rest of the markers. **(m)** Survival curves for CRC patients with high/low CD177$^+$ Treg cells infiltration in TCGA cohort. Data are represented as mean ± SEM and were analysed by the paired Student's *t*-test **(a–k)**. Kaplan–Meier curves were generated by the log-rank Mantel–Cox test **(m)**. *******P* < 0.01, ***P < 0.001, ****P < 0.0001. NS, not significant.

CD177^{+} Treg cells were activated (Figure 3e and f).[10,33] In addition, CD177^{+} Treg cells had higher levels of most immune checkpoint molecules than CD177^{−} Treg cells, including GITR, OX40, CTLA-4, CD39 and TIM3 (Figure 3g–k), implying that CD177^{+} Treg cells may be more activated and immunosuppressive.[6,34] However, PD-1 expression levels on CD177^{+} Treg cells were relatively low (Figure 3l). Moreover, according to survival analysis using data from The Cancer Genome Atlas (TCGA) database, CD177^{+} Treg cell enrichment was associated with a shorter overall survival (OS) time in patients with CRC (Figure 3m). These results suggested that CD177^{+} Treg cells are an essential component of the TME and may be potential therapeutic target for CRC.

Difficulty in inducing CD177 expression in Treg cells *in vitro*

Originally, we wanted to study the role of CD177 in Treg cells. However, CD177 was infrequently observed in induced Treg (iTreg) cells and its expression on natural Treg (nTreg) cells was minimal (Supplementary figure 4a and b). Furthermore, it was difficult to upregulate CD177 expression in Treg cells. We attempted to induce the expression of CD177 in Treg cells by adding different stimulating factors, including inflammatory cytokines commonly found in the TME (TNF-α and IL1β), tumor supernatants, CD177-induced factors on neutrophils (G-CSF and GM-CSF), vascular endothelial growth factor, IC ligand (GITRL), IL-2 and TGF-β, into the cell culture medium. However, none of these approaches were effective (Supplementary figure 4c and d). Although tumor supernatants slightly upregulated the CD177 MFI, the positivity rate of CD177 remained unchanged (Supplementary figure 4e).

CD177 promoted the transendothelial migration of T cells

CD177 drives neutrophil transmigration by binding to PECAM-1 in the vascular endothelium.[22] We speculated that CD177^{+} Treg cells have a similar phenotype. Immunofluorescence (IF) was used to locate CD177^{+} Treg cells and blood vessels in CRC tumor samples. The results showed that CD177^{+} Treg cells resided close to the vasculature in the TME (Figure 4a). Moreover, the percentage of peripheral CD177^{+} Treg cells was higher in patients than in healthy donors (Figure 4b). Thus, we hypothesised that CD177 promotes the diffusion of Treg cells into the blood or peritumor tissues, leading to tumor proliferation and metastasis. To verify this hypothesis, we designed the lentiviral plasmid pHR-CD177-SFFV-IRES-EGFP (Figure 4c). After lentiviral packaging and infection, iTreg cells labelled with EGFP were selected by flow cytometry (Figure 4d). The infection efficiency and expression of CD177 are shown in Supplementary figure 4f and g. Selected iTreg cells were used for the transendothelial migration assays after expanding for 2 days *in vitro*. Human umbilical vein endothelial cells (HUVECs), which have high PECAM-1 expression levels, were used to simulate blood vessels in the TME (Figure 4e). We verified that HUVECs significantly inhibited iTreg cells migration (Supplementary figure 4h). CCL19 and CCL22 were used to recruit iTreg cells during the assay. The results demonstrated that CD177-overexpressing (CD177-OE) iTreg cells migrated through the HUVEC monolayer faster than empty-vector-control (EV)-infected iTreg cells (Figure 4f). This process was blocked by an anti-CD177 monoclonal antibody (mAb) and an anti-PECAM-1 mAb (Figure 4g). In contrast, both the mAbs rarely interrupted EV-iTreg cell migration (Figure 4h). Unexpectedly, CD177 overexpression downregulated PD-1 expression on iTreg cells, which was consistent with the low PD-1 expression levels on intratumoral CD177^{+} Treg cells (Figures 3l and 4i). Furthermore, CD177-OE CD8^{+} T cells exhibited a similar phenotype of transendothelial migration, suggesting that the overexpression of CD177 may serve as a valuable strategy to enhance CAR-T cells transendothelial migration (Figure 4j).

DISCUSSION

Although progress has been made in the treatment of CRC to inhibit tumor progression and metastasis, it remains the third most common malignant cancer. Previous studies have shown that the inherent heterogeneity and immune milieu of CRC poses challenges to the potency of immune checkpoint blockade therapy.[35,36] Therefore, identifying efficient targets is critical for future CRC treatments. Increased numbers of activated Treg cells appear to correlate with poor oncological outcomes in various types of cancer. However, the exact function of these cells in CRC remains unclear. Some studies have suggested
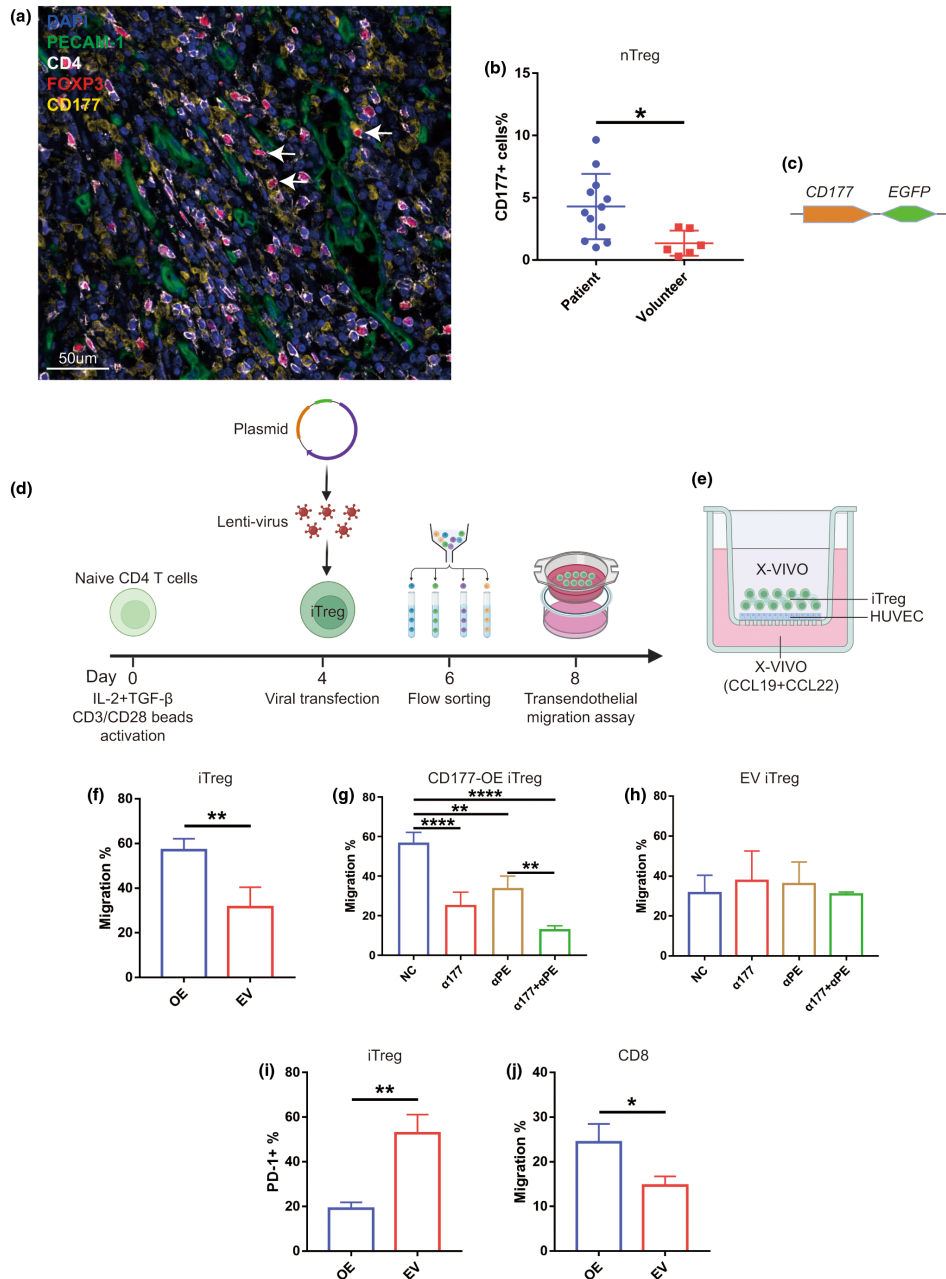
Figure 4. CD177 promotes T-cell transendothelial migration. **(a)** Human colorectal cancer (CRC) specimens were stained with DAPI (blue), PEACM-1 (green), CD4 (white), FOXP3 (red) and CD177 (yellow), respectively. The scale bar (50 μm) is placed at the left corner of each image. **(b)** CD177+ Treg cells in peripheral blood mononuclear cells from CRC patients ($n = 12$) and healthy volunteers ($n = 6$). **(c)** Diagram of CD177-EGFP in pHR plasmid. **(d)** Model of iTreg cells induction, transfection, selection and then expanded for 2 days before the assay. **(e)** Diagram of the transendothelial migration assay. HUVECs were seeded on the upper surface of the transwell insert and iTreg cells were placed in the upper chamber filled with X-VIVO. The lower chamber was filled with X-VIVO containing CCL19 and CCL22 (200 ng mL^{-1}). **(f)** Migration rate of OE iTreg cells and EV iTreg cells after 4 h. OE: CD177-overexpression; EV: empty vector control. **(g)** Migration rate of OE iTreg cells at 4 h under different treatments. NC, negative control; α177, anti-CD177; αPE, anti-PECAM-1. **(h)** Migration rate of EV iTreg cells after 4 h under different treatments. **(i)** PD-1 expression of OE iTreg cells and EV iTreg cells. **(j)** Migration rate of OE CD8+ T cells and EV CD8+ T cells at 4 h. The lower chamber was filled with X-VIVO containing CCL3 (200 ng mL^{-1}) in **(j)**. Data are represented as mean ± SEM and were analysed by the unpaired Student's *t*-test **(b, f, i, j)** or one-way ANOVA **(g, h)**. *$P < 0.05$, **$P < 0.01$, ****$P < 0.0001$. Data are pooled from three independent experiments.

that infiltrating Treg cells have adverse prognostic implications,[37] whereas earlier studies suggested a positive association with CRC prognosis.[38] Recently, the heterogeneity of tumor-infiltrating Treg cells has been elucidated using scRNA-seq, which may explain the inconsistencies observed in previous studies.[27]

Previous studies on CD177 have focussed on its functions in neutrophil migration and its bactericidal activities.[39,40] However, the role of CD177 in Treg cells, particularly tumor-infiltrating Treg cells in CRC, remains unclear. In this study, we analysed scRNA-seq data from CRC patients and identified CD177^{+} Treg cell enrichment in the TME (Figure 1 and Supplementary figure 1). Combined with flow cytometry analysis, CD177 was found to be highly expressed by Treg cells, especially intratumoral Treg cells (Figure 2). Subsequent analysis revealed that CD177^{+} Treg cells were more activated and possessed a stronger immunosuppressive phenotype (Figure 3). Simultaneously, the co-expression of CD177 with CCR8 and alternate ICs indicated its suitability for combination therapy or bispecific antibody design.[41] Furthermore, survival analysis revealed that a high density of CD177^{+} Treg cells was associated with a poor prognosis in patients with CRC (Figure 3m). PD-1, a member of the co-inhibitory IC family, suppresses T-cell activity upon PD-L1 activation.[42] Unlike other ICs, our results demonstrated that CD177^{+} Treg cells exhibited decreased PD-1 expression levels (Figure 3l), which was also observed in CD177-OE iTreg cells (Figure 4i). This led us to hypothesise that CD177 may partially influence PD-1 expression, thereby preventing Treg cells from engaging in PD-1/PD-L1 signalling. Finally, we confirmed that CD177 enhanced Treg cell transmigration by binding to PECAM-1 (Figure 4f–h), which may account for the elevated levels of CD177^{+} Treg cells in PBMCs from patients with CRC.

Recently, CAR-T cell therapy has demonstrated remarkable efficacy in the treatment of haematological malignancies and has provided a new direction for the treatment of solid tumors.[43] However, CAR-T cell therapy for solid tumors still faces challenges. One reason for this is the abnormal vasculature of the TME. The downregulation of intercellular adhesion molecule-1 (ICAM-1) and vascular cell adhesion molecule-1 (VCAM-1) in vascular endothelial cells leads to ineffective T-cell adhesion and infiltration of T cells.[43,44] Unlike ICAM-1 and VCAM-1, PECAM-1 is a classical marker of blood vessels that

exhibits elevated expression levels in human CRC tumor tissues (Figure 4a). Moreover, we observed stronger endothelial migration capability in CD177-OE CD8^{+} T cells (Figure 4j). Our findings suggest the potential benefit of combining CD177 overexpression with CAR-T cell therapy to overcome the blockade of aberrant intratumoral vasculature. Notably, CD177 does not possess signal transduction capabilities and has little impact on CAR-T cell function.[45]

Our findings revealed a correlation between CD177 and the expression profile of inhibitory molecules, as well as the enhanced transendothelial capacity of human tumor-infiltrating Treg cells. However, the mechanism by which CD177 regulates Treg cell infiltration and function remains unclear. As a classic surface protein associated with cell migration, CD177 lacks an intracellular domain, suggesting that CD177 may have difficulty in regulating complex downstream signalling on its own. Therefore, the actual function of CD177 may involve a set of mechanisms that promote cell–cell contact or migration.[39] Previous studies of tumor-infiltrating CD177^{+} Treg cells have predominantly focussed on transcriptomic data and clinical specimens. Additional *in vivo* experiments are necessary to elucidate the function of CD177^{+} Treg cells and the mechanisms by which CD177 influences the migration and inhibition of Treg cells.[26]

In summary, our study showed that CD177^{+} Treg cells are enriched in human CRC. These Treg cells tended to be more immunosuppressive in the TME and were associated with a poor prognosis in patients with CRC. In addition, we confirmed that CD177 overexpression augmented the transendothelial migration capacity of both Treg cells and CD8^{+} T cells, which potentially offers significant benefits in adoptive cell immunotherapy.

METHODS

Unsupervised clustering and marker identification

The digital expression matrices were imported into the Seurat (4.4.0) for standard downstream pipeline analysis. Low-quality cells were filtered out if their library size or the number of expressed genes fell below predefined thresholds. Both thresholds were defined as the median of all cells minus or plus $3\times$ the median absolute deviation. First, the data were normalised and scaled. Principal component analysis (PCA) of 2000 genes, variably expressed across all 160 865 cells, was performed. Subsequently,

Harmony was used to remove and mitigate batch effects from different samples and to generate the neighbour graph with parameter n pcs set to 35. We then used Uniform Manifold Approximation and Projection (UMAP) to embed the graph in two dimensions and the Leiden graph-clustering to cluster the neighbourhood graph of cells with resolution parameter equal to 1. These processes identified several cell populations that were readily classified into known cell lines using marker genes.

Differentially expressed gene analysis

To identify feature genes that distinguish CD177$^+$ from CD177$^-$ Treg cells, differential expression analysis was performed using the 'FindMarkers' function implemented in the Seurat package. The criteria for significant differential expression were set as log-scaled fold change ≥ 0.25 and the adjusted *P*-value < 0.05 (Wilcoxon Rank Sum test). Differentially expressed genes meeting the criteria are listed in Supplementary table 1.

Ethics approval and consent to participate

A total of 21 patients, pathologically diagnosed with CRC at Renji Hospital Shanghai Jiao Tong University, were enroled in this study. Paired fresh tumor, peritumoral tissue samples and peripheral blood samples were collected. Detailed clinical and pathological information including age, gender and tumor size are listed in Supplementary table 2. Peripheral and tissue-infiltrating immune cells were isolated from blood and tumor samples for analysis via flow cytometry.

We excluded patients who (1) had recurrent CRC after radical surgery, (2) received neoadjuvant chemotherapy or radiotherapy previously, (3) suffered from other malignant tumors and (4) had autoimmune or immunodeficiency diseases. Tumor TNM stage was determined based on the pathological tumor, node and metastasis staging according to the American Joint Committee on Cancer (AJCC 8th edition) staging system.

All patients were given informed consent for the collection of clinical information, tissue collection, and research testing under Institutional Review Board (IRB)-approved protocols (2017-114-CR-02 and KY2022-174-B) at Renji Hospital Shanghai Jiao Tong University.

Cell isolation

Fresh tissue samples were surgically removed from the patients and immersed in a complete medium containing 90% Dulbecco's modified eagle medium (DMEM; Catalogue #11054001, GIBCO) and 10% fetal bovine serum (FBS; Catalogue #16140071, GIBCO). Samples were transported to the laboratory in a refrigerated container within 4 h. Tissues were cut into pieces (1–3 mm in diameter) and incubated in 3 mL of complete medium containing 2 mg mL^{-1} type IV collagenase (Catalogue #C5138, Sigma) and 50 U mL^{-1} DNase I (Catalogue #DN25, Sigma) for 40 min at 37°C on a shaker (200 rpm). Then, the dissociated cell suspensions were filtered through 50-μm nylon meshes to obtain single-cell suspensions. Peripheral blood mononuclear cells were isolated by density gradient centrifugation (speed at 2000 rpm; Acceleration ramp 3 and Braking ramp 0) for 20 min using Ficoll–Paque Plus (Catalogue #17-1440-03-1, GE Healthcare).

Flow cytometry and sorting

Single-cell suspensions were then stained with various fluorochrome-conjugated antibodies (as shown in Supplementary table 3) in FACS buffer (PBS containing 2% FBS). After washing with FACS buffer, cells were incubated for 30 min at 4°C in the dark for surface markers staining, and dead cells were labelled with Fixable Viability Dye (Catalogue #65-0865-14, eBioscience). Cells were then fixed and permeabilised with fixation/permeabilisation concentrate (Catalogue #00-5521-00, eBioscience) for 40 min at room temperature (22–24°C) in the dark. Intracellular targets were stained for 40 min at 4°C in the dark, followed by two wash steps with permeabilisation buffer (Catalogue #00-8333-56, eBioscience). For sample acquisition, a BD LSRFortessa X-20 cell analyser embedded with the FACS DIVA software (BD Bioscience) was used. Results were analysed with FlowJo v10 (FlowJo LLC).

Regarding flow sorting, after being stained and labelled with Fixable Viability Dye, EGFP$^+$ iTreg cells were sorted on FITC channel using a BD FACSAria III (BD Biosciences). Human PBMCs were isolated from the peripheral blood of CRC patients or healthy donors. The nTreg cells (CD4$^+$CD25^{high}CD127^{low}) were sorted by BD FACSAria II cell sorter.

Multiplexed immunofluorescence staining (tyramide signal amplification, TSA)

Multiplex staining was performed using a PANO 7-plex IHC kit (Catalogue #0004100100, Panovue) according to the manufacturer's instructions. CD4, FOXP3, PECAM-1, and CD177 antibodies were sequentially applied, followed by horseradish peroxidase-conjugated secondary antibody incubation and tyramide signal amplification. The slides were microwave heat treated after each tyramide signal amplification. Nuclei were stained with DAPI after all the antigens above had been labelled. The stained slides were scanned to obtain multispectral images using the Mantra System (PerkinElmer), which captured the fluorescent spectra at 20-nm wavelength intervals from 420 to 720 nm with identical exposure times.

Survival analysis

We analysed the association of CD177$^+$ Treg cell density and OS in TCGA cohort. For survival analysis, the samples in the database were divided into high and low expression groups based on the mean expression of feature genes. We analysed the gene signature of CD177$^+$ Treg cells and CD177$^-$ Treg cells from the scRNA-seq data of CRC (obtained from GSE108989). The optimal cut-off value was calculated using survminer (0.4.9). Kaplan–Meier survival curves were then plotted to show the differences in survival time. The package survival (3.5.7) was used to determine the statistical significance of the log-rank *P*-values, reported by the Cox regression models. The

In vitro cell culture

Human CD4+ CD25lo CD45RAhi naive T cells were flow sorted from the PBMCs of healthy donors using BD FACSAria II (BD Bioscience). Cells were differentiated into iTreg cells using anti-CD3/CD28 DynaBeads (Catalogue #11132D, GIBCO) at a 1:4 bead-to-cell ratio in cell culture medium [X-VIVO (Catalogue #04-418Q, Lonza), supplemented with 10% FBS (Catalogue #10100147C, GIBCO), 1% L-Glutamine-100× (Catalogue #335050061, GIBCO), 1% MEM Non-Essential Amino Acids-100× (Catalogue #11140050, GIBCO), 1 mM sodium pyruvate (Catalogue #11360070, GIBCO), 1% Antibiotic-Antimycotic 100× (Catalogue #15240112, GIBCO)], 100 U mL^{-1} rhIL-2 (Catalogue #200-02, Peprotech) and 5 ng mL^{-1} hTGF-β1 (Catalogue #7754-BH-100/CF, R&D).

Human umbilical vein endothelial cells (HUVEC), isolated from the vein of the umbilical cord, were purchased from ZQXZbio (Catalogue #DFSC-EC-01) and cultured in Endothelial Cell Growth Medium (Catalogue #C-22010, Sciencell). Cell culture dishes should be pre-coated with 100 μg mL^{-1} fibronectin (Catalogue #CSP044, ZQXZbio) for 1 h at 37°C or overnight at 4°C before seeding the HUVECs.

All experiments were performed with mycoplasma-free cells.

Lentivirus construction and infection

For the migration assay, CD177 was cloned into pHR lentiviral vector (pHR-SFFV-IRES-EGFP). Then, pHR-CD177-SFFV-IRES-EGFP or pHR-SFFV-IRES-EGFP, delta8.9 and pMD2.G were co-transfected with polyethyleneimine reagent (Catalogue #23966, Polyscience) into HEK293T cells when the cells reached 70% confluence in 10-cm cell culture dishes.

The supernatants containing viruses were harvested at 48- and 72-h post-transfection and concentrated using centrifugal filters (Catalogue #UFC9100, MERCK). Before infection, human iTreg cells were expanded for 3 days in a 48-well plate. Next, iTreg cells were diluted into 1 million cells per well, followed by the addition of lentiviruses and 8 μg mL^{-1} polybrene (Catalogue #TR-1003, Sigma-Aldrich). Then, the 48-well plate was centrifuged at 2500 rpm for 90 min at 32°C, followed by incubation at 37°C with 5% CO$_2$. The virus was removed after 24 h.

Transendothelial migration assays

300 μL HUVEC (1×10^5 cells mL^{-1}) cells were cultured on 6.5-mm transwells with 5-mm pore sizes (Catalogue #CLS3421, Sigma-Aldrich). The transwells were first coated with 100 μg mL^{-1} fibronectin before culturing HUVEC cells on the inserts. Next, 600 μL X-VIVO medium containing CCL19 and CCL21 (200 ng mL^{-1}, Cat#300-29B and 300-36A, Peprotech) or CCL3 (200 ng mL^{-1}, Cat#11292-H08Y, SinoBiological) were placed in the lower chamber. Then, 300 μL of iTreg or CD8+ T cells (1×10^5 cells), resuspended in X-VIVO medium, were loaded into the upper chamber and allowed to transmigrate for 4 h at 37°C. The number of migrated cells was determined by a haemocytometer, and data were expressed as the percentage of migration compared with loaded cells.

Statistical analyses

Comparisons of the percentages of different T cell types between the tumor and peritumor tissues in the scRNA-seq data were calculated using the Student's *t*-test. Other statistical analyses were performed using SPSS 23.0 and GraphPad Prism 8.0. The Student's *t*-test or one-way ANOVA was used to compare two or more independent conditions. Pearson's correlation analysis and linear regression analysis were used to assess correlations between variables. All *P*-values were two-tailed, and *P*-values < 0.05 were considered statistically significant.

AUTHOR CONTRIBUTIONS

Shouyu Ke: Conceptualization; data curation; formal analysis; investigation; resources; writing – original draft. **Yi Lei:** Data curation; formal analysis; resources; software; visualization. **Yixian Guo:** Conceptualization; investigation; methodology; resources. **Feng Xie:** Conceptualization; methodology; software; validation; visualization. **Yimeng Yu:** Data curation; resources; validation. **Haigang Geng:** Investigation; resources. **Yiqing Zhong:** Investigation; resources. **Danhua Xu:** Funding acquisition; resources. **Xu Liu:** Funding acquisition; methodology; resources. **Fengrong Yu:** Investigation; resources. **Xiang Xia:** Investigation; resources. **Zizhen Zhang:** Funding acquisition; resources. **Chunchao Zhu:** Funding acquisition; resources. **Wei Ling:** Investigation; resources. **Bin Li:** Conceptualization; funding acquisition; methodology; project administration; supervision; writing – review and editing. **Wenyi Zhao:** Conceptualization; project administration; supervision; writing – review and editing.

CONFLICT OF INTEREST

The authors declare no competing interests.

DATA AVAILABILITY STATEMENT

The processed CRC public scRNA-seq data set were downloaded from GEO (accession GSE108989 and

GSE178341). Public bulk RNA-seq data sets were downloaded from TCGA database. All the transcriptomic data were obtained and analysed according to the requirements and guidelines of the providers.

REFERENCES

1. Sung H, Ferlay J, Siegel RL et al. Global cancer statistics 2020: GLOBOCAN estimates of incidence and mortality worldwide for 36 cancers in 185 countries. *CA Cancer J Clin* 2021; **71**: 209–249.
2. Dekker E, Tanis PJ, Vleugels JLA, Kasi PM, Wallace MB. Colorectal cancer. *Lancet* 2019; **394**: 1467–1480.
3. Bando H, Ohtsu A, Yoshino T. Therapeutic landscape and future direction of metastatic colorectal cancer. *Nat Rev Gastroenterol Hepatol* 2023; **20**: 306–322.
4. van Morris K, Kennedy EB, Baxter NN et al. Treatment of metastatic colorectal cancer: ASCO guideline. *J Clin Oncol* 2023; **41**: 678–700.
5. Pardoll DM. The blockade of immune checkpoints in cancer immunotherapy. *Nat Rev Cancer* 2012; **12**: 252–264.
6. Kraehenbuehl L, Weng C-H, Eghbali S, Wolchok JD, Merghoub T. Enhancing immunotherapy in cancer by targeting emerging immunomodulatory pathways. *Nat Rev Clin Oncol* 2022; **19**: 37–50.
7. Fidelle M, Yonekura S, Picard M et al. Resolving the paradox of colon cancer through the integration of genetics, immunology, and the microbiota. *Front Immunol* 2020; **11**: 600886.
8. Chen Y, Zheng X, Wu C. The role of the tumor microenvironment and treatment strategies in colorectal cancer. *Front Immunol* 2021; **12**: 792691.
9. Xiao Y, Yu D. Tumor microenvironment as a therapeutic target in cancer. *Pharmacol Ther* 2021; **221**: 107753.
10. Hori S, Nomura T, Sakaguchi S. Control of regulatory T cell development by the transcription factor Foxp3. *Science* 2003; **299**: 1057–1061.
11. Li Z, Li D, Tsun A, Li B. FOXP3⁺ regulatory T cells and their functional regulation. *Cell Mol Immunol* 2015; **12**: 558–565.
12. Sawant DV, Yano H, Chikina M et al. Adaptive plasticity of IL-10⁺ and IL-35⁺ Treg cells cooperatively promotes tumor T cell exhaustion. *Nat Immunol* 2019; **20**: 724–735.
13. Togashi Y, Shitara K, Nishikawa H. Regulatory T cells in cancer immunosuppression – implications for anticancer therapy. *Nat Rev Clin Oncol* 2019; **16**: 356–371.
14. Tanaka A, Sakaguchi S. Regulatory T cells in cancer immunotherapy. *Cell Res* 2017; **27**: 109–118.
15. Adamczyk A, Pastille E, Kehrmann J et al. GPR15 facilitates recruitment of regulatory T cells to promote colorectal cancer. *Cancer Res* 2021; **81**: 2970–2982.
16. Lu Y, Li Y, Liu Q et al. MondoA-thioredoxin-interacting protein axis maintains regulatory T-cell identity and function in colorectal cancer microenvironment. *Gastroenterology* 2021; **161**: 575–591.
17. Goldschmeding R, van Dalen CM, Faber N et al. Further characterization of the NB 1 antigen as a variably expressed 56-62 kD GPI-linked glycoprotein of plasma membranes and specific granules of neutrophils. *Br J Haematol* 1992; **81**: 336–345.
18. Stroncek DF, Caruccio L, Bettinotti M. CD177: A member of the Ly-6 gene superfamily involved with neutrophil proliferation and polycythemia vera. *J Transl Med* 2004; **2**: 8.
19. Stroncek D. Neutrophil-specific antigen HNA-2a (NB1, CD177): Serology, biochemistry, and molecular biology. *Vox Sang* 2002; **83**: 359–361.
20. Stroncek DF, Shankar RA, Noren PA, Herr GP, Clement LT. Analysis of the expression of NB1 antigen using two monoclonal antibodies. *Transfusion* 1996; **36**: 168–174.
21. Stroncek DF. Neutrophil-specific antigen HNA-2a, NB1 glycoprotein, and CD177. *Curr Opin Hematol* 2007; **14**: 688–693.
22. Sachs UJH, Andrei-Selmer CL, Maniar A et al. The neutrophil-specific antigen CD177 is a counter-receptor for platelet endothelial cell adhesion molecule-1 (CD31). *J Biol Chem* 2007; **282**: 23603–23612.
23. Zhou G, Yu L, Fang L et al. CD177⁺ neutrophils as functionally activated neutrophils negatively regulate IBD. *Gut* 2018; **67**: 1052–1063.
24. Plitas G, Konopacki C, Wu K et al. Regulatory T cells exhibit distinct features in human breast cancer. *Immunity* 2016; **45**: 1122–1134.
25. Simone M, Arrigoni A, Rossetti G et al. Transcriptional landscape of human tissue lymphocytes unveils uniqueness of tumor-infiltrating T regulatory cells. *Immunity* 2016; **45**: 1135–1147.
26. Kim M-C, Borcherding N, Ahmed KK et al. CD177 modulates the function and homeostasis of tumor-infiltrating regulatory T cells. *Nat Commun* 2021; **12**: 5764.
27. Zhang L, Yu X, Zheng L et al. Lineage tracking reveals dynamic relationships of T cells in colorectal cancer. *Nature* 2018; **564**: 268–272.
28. Pelka K, Hofree M, Chen JH et al. Spatially organized multicellular immune hubs in human colorectal cancer. *Cell* 2021; **184**: 4734–4752.
29. Shevach EM, Thornton AM. tTregs, pTregs, and iTregs: Similarities and differences. *Immunol Rev* 2014; **259**: 88–102.
30. Akimova T, Beier UH, Wang L, Levine MH, Hancock WW. Helios expression is a marker of T cell activation and proliferation. *PLoS One* 2011; **6**: e24226.
31. Chen D, Bromberg JS. T regulatory cells and migration. *Am J Transplant* 2006; **6**: 1518–1523.
32. Korbecki J, Grochans S, Gutowska I, Barczak K, Baranowska-Bosiacka I. CC chemokines in a tumor: A review of pro-cancer and anti-cancer properties of receptors CCR5, CCR6, CCR7, CCR8, CCR9, and CCR10 ligands. *Int J Mol Sci* 2020; **21**: 7619.
33. Sakaguchi S, Sakaguchi N, Asano M, Itoh M, Toda M. Immunologic self-tolerance maintained by activated T cells expressing IL-2 receptor alpha-chains (CD25). Breakdown of a single mechanism of self-tolerance causes various autoimmune diseases. *J Immunol* 1995; **155**: 1151–1164.
34. Timperi E, Barnaba V. CD39 regulation and functions in T cells. *Int J Mol Sci* 2021; **22**: 8068.
35. Sharma P, Hu-Lieskovan S, Wargo JA, Ribas A. Primary, adaptive, and acquired resistance to cancer immunotherapy. *Cell* 2017; **168**: 707–723.

36. Liao W, Overman MJ, Boutin AT *et al*. KRAS-IRF2 axis drives immune suppression and immune therapy resistance in colorectal cancer. *Cancer Cell* 2019; **35**: 559–572.

37. Ahmadzadeh M, Pasetto A, Jia L *et al*. Tumor-infiltrating human CD4^{+} regulatory T cells display a distinct TCR repertoire and exhibit tumor and neoantigen reactivity. *Sci Immunol* 2019; **4**: eaao4310.

38. Salama P, Phillips M, Grieu F *et al*. Tumor-infiltrating FOXP3^{+} T regulatory cells show strong prognostic significance in colorectal cancer. *J Clin Oncol* 2009; **27**: 186–192.

39. Bai M, Grieshaber-Bouyer R, Wang J *et al*. CD177 modulates human neutrophil migration through activation-mediated integrin and chemoreceptor regulation. *Blood* 2017; **130**: 2092–2100.

40. Zhang R, Su L, Fu M *et al*. CD177^{+} cells produce neutrophil extracellular traps that promote biliary atresia. *J Hepatol* 2022; **77**: 1299–1310.

41. Kidani Y, Nogami W, Yasumizu Y *et al*. CCR8-targeted specific depletion of clonally expanded Treg cells in tumor tissues evokes potent tumor immunity with long-lasting memory. *Proc Natl Acad Sci USA* 2022; **119**: e2114282119.

42. Keir ME, Butte MJ, Freeman GJ, Sharpe AH. PD-1 and its ligands in tolerance and immunity. *Annu Rev Immunol* 2008; **26**: 677–704.

43. Liu G, Rui W, Zhao X, Lin X. Enhancing CAR-T cell efficacy in solid tumors by targeting the tumor microenvironment. *Cell Mol Immunol* 2021; **18**: 1085–1095.

44. Buckanovich RJ, Facciabene A, Kim S *et al*. Endothelin B receptor mediates the endothelial barrier to T cell homing to tumors and disables immune therapy. *Nat Med* 2008; **14**: 28–36.

45. Hu N, Westra J, Kallenberg CGM. Membrane-bound proteinase 3 and its receptors: Relevance for the pathogenesis of Wegener's granulomatosis. *Autoimmun Rev* 2009; **8**: 510–514.

Supporting Information

Additional supporting information may be found online in the Supporting Information section at the end of the article.